Journal of Materials and Environmental Science
ISSN : 2028-2508
CODEN : JMESCN

J. Mater. Environ. Sci., 2020, Volume 11, Issue 8, Page 1386-1402

http://www.jmaterenvironsci.com

Bis thiourea phthalato Cobalt (II) complex: synthesis and studying as corrosion inhibitors for carbon steel alloy(C1010) in 0.1M HCl

Israa M. Al-Jubanawi [1], Hadi Z. Al-Sawaad [2] , Ahmed A. AlWaaly [3]

[1]Ministry of Education, Mayssan's Directorate of Education
[2,3]University of Basrah, College of Science, Department of Chemistry

Received 02 July 2020
Revised 24 July 2020
Accepted 25 July 2020

Keywords
- ✓ *thiourea complexes,*
- ✓ *phthalic acid complexes,*
- ✓ *corrosion inhibitors,*
- ✓ *cobalt complexes,*
- ✓ *carbon steel,*
- ✓ *acidic corrosive medium*

hadiziara@yahoo.com
Phone: +9647801131734
ahmed.alwaaly@me.com.
Phone:+9647726663831

Abstract

In this study of bis thiourea phthalato cobalt (II)complex (PTUCo) was synthesized and characterized by CHNS, FTIR, UV-Visible, Mass, TG and XRD techniques. The complex was evaluated as corrosion inhibitor for carbon steel alloy (C1010) against corrosive medium of 0.1M hydrochloric acid at 25ºC and showed the efficiency 95.63% at concentration of 5 ppm. The effect of temperature on the inhibition behavior was studied at 35, 45 and 55 ºC and the inhibitor reveals reducing in its efficiency as temperature raised, kinetic parameters like E_a , ΔH* and ΔS* were calculated and depicted that increasing the activation of energy in presence of the inhibitor compared with the absence of the inhibitor. The inhibitor behaves as mixed inhibitor. The adsorption study insist that the inhibitor obey to Langmuir adsorption isotherm.

1. Introduction

Metals in general are widely used in industry, especially carbon steel which is considered as a material of choice, in addition it is often used as a construction material for chemical reactors, heat exchange systems and boiler, storage tanks, oil and gas transportation pipelines[1, 2] Metals require a pretreatment most of the time based on acidic solutions such as hydrochloric acid solution which is widely used in the industry: cleaning, stripping, acidification of oil, descaling and petrochemical processes. In the oil industry, 15% HCl is used for the acidification treatment, to solubilize the manipulations [3-5]. Metal's corrosion is an unavoidable difficulty for industries. In fact, corrosion occurs either by the two different metals or alloys, and also if that metal or alloy is present in corrosive environments, such as saline, basic or acidic media. [6,7]. Mild steel is the most extensively employed metal in industrial applications because of its excellent mechanical characteristics and inexpensiveness [8]. To treat the corrosion problems, there are several ways, one of them is used the corrosion inhibitors, For this, the using of inhibitor is one of the most trustworthy and economical method , that are chemicals when added in a suitable concentration are able to reduce the corrosion rate when present in the corrosion system without significantly changing the concentration of any other corrosive agent. The use of inhibitors during acid pickling procedure is one of the most practical methods for protection against corrosion in acidic media as well. Organic compounds containing hetero-atoms like N, O, S and P are famous compounds that

used as corrosion inhibitors for iron and its alloys especially for carbon steel alloy as for reduction of acid consumption occurring during the course of corrosion [9, 10]. Although, a great number of studies devoted to the subject of corrosion inhibitors, the development of corrosion inhibitors has always determined by their effectiveness ,the complexes are tried to use as corrosion inhibitors for carbon steel alloy from many researchers [11-27]. thiourea, its derivatives and its complexes were used as corrosion inhibitors in industrial operations [28, 29]. In the present work, a novel complex bis thiourea phthalato cobalt(II) complex was synthesized to estimate as corrosion inhibitor against corrosive environment of 0.1M HCl on the carbon steel alloy C1010 surface.

2. Material and Methods

2.1. Chemicals

The chemicals that used in this study were purchased from different companies, including: Ethanol(99.99 Scharlau), Hydrochloric acid(37Aldrich), Dimethyl sulfoxide (DMSO 99 Alpha), Dichloride methane(DCM 99 Fluka), Di ethyl ether (99.5 SCH), thiourea (99.99 Aldrich), Cobalt chloride($CoCl_2.6H_2O$ 99.5GPR), Phthalic anhydride(99.5 GPR) .

2.2 Synthesis of bis thiourea phthalato cobalt (II) complex (PTUCo).

To a solution of $CoCl_2.6H_2O$ (10 g, 0.042 mol) in 100 mL of ethanol was added thiourea (6.384 g, 0.0.084 mol) dropwise. After the solution was reflux for 2h, a solution of phthalic anhydride (6.216 g, 0.042 mol) and sodium hydroxide (3.36 g, 0.084 mol) in 40 mL of water was added. The mixture was stirrer for 18h and after cooling the violet precipitate filtrated and washed by distilled water, absolute ethanol and diethyl ether. Washing of the complex was achieved by dissolving the solid with a minimum amount of dichloromethane and then adding a large access of ethanol [30]. Leaving the solution undisturbed at room temperature for 24 h produced brown precipitate which were dried in vacuum. The melting point of the product is (<300℃ decoms) violet color, Mwt (374.633g.mol^{-1}), Yield:4.1637g (26%). [31, 32]. Scheme (1) show the synthesis of the complex.

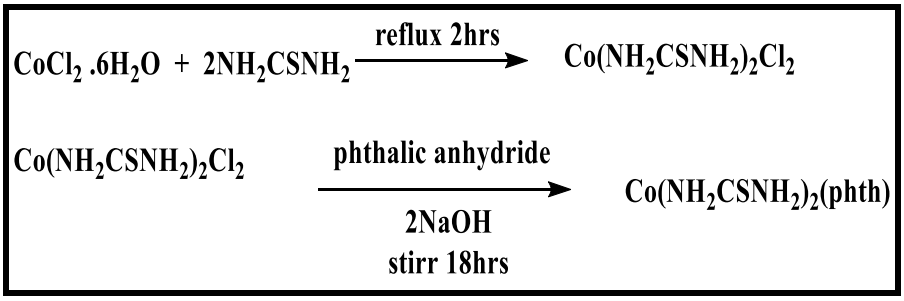

Scheme (1): Shows the Synthesis of PTUCo complex.

3. Characterization of the bis thiourea phthalato cobalt (II)complex (PTUCo):

3.1. *CHNS Element analysis:* The complex PTUCo was characterized by CHNS technique and the data shows matching between theoretical calculation and experimental, Table 2 show CHNS of complex.

Table 1 . CHN Element analysis of PTUCo

Co $C_{10}H_{12}O_4S_2N_4$	C%	H%	N%	S%
Calculated	32.03	3.20	14.94	17.08
Found	32.01	3.21	14.88	17.05

3.2. FTIR spectroscopy:

the complex PTUCo was characterized by FTIR technique (KBr pellet, cm^{-1})in the region(400-4000 cm^{-1}), the complex was given the following packages υ_{NH}(3502)(assym), 3417 (symm), $\upsilon_{C=O}$ (1688), υ_{NH} (1566) (bending)),(1612) $\upsilon_{C=C(aromatic)}$, υ_{COO}(2200), $\upsilon_{C=S}$(1411), υ_{C-O}(1153) ,and υ_{CN} (1489) , υ_{C-S}(756) and out of plane bending υ_{N-H}(702), υ_{Co-S}(493), υ_{Co-O}(705) [33-38]. Figure 1 show FTIR spectrum for PTUCo

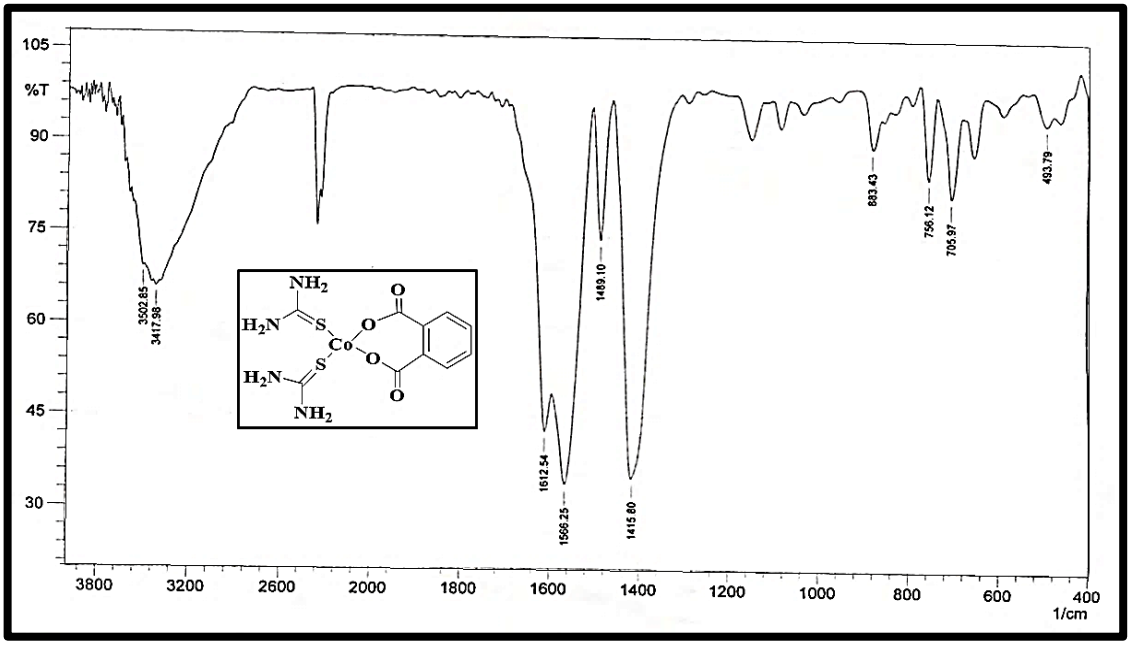

Figure (1): FTIR spectrum for PTUCo complex.

3.3. UV-Visible PTUCo complex:

The complex PTUCo was characterized by UV-Visible as shown in Figure 2 below where, Figure 2 revealed four transitions, 290 nm can be assigned to π→π* and n→π* in benzene ring and the two carboxylic groups that they ortho position one to another respectively. While the transition 335 nm is assigned to n→π* for C=S group and 405,435,580nm is assigned to d-d transitions [33, 39-41].

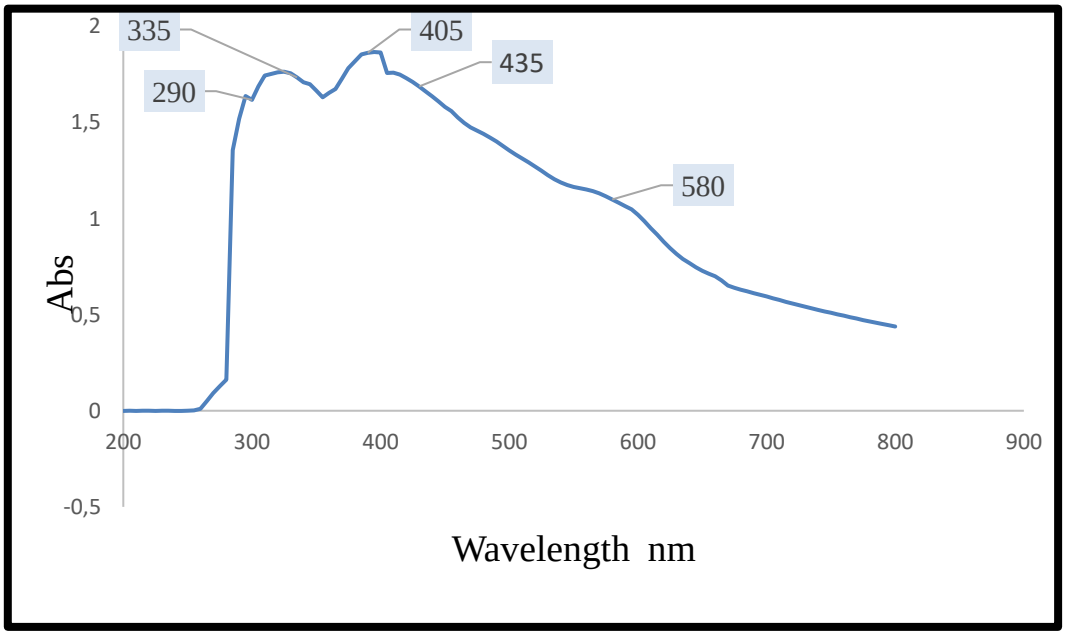

Figure 2: UV-Visible spectrum PTUCo complex.

3.4. Magnetic Susceptibility:

The magnetic moment of a complex was calculated and found to be equal μeef 3.9, where magnetic sensitivity calculations proved that the tetrahedral and cobalt oxidation state (2+) Co^{2+}. Table 2 that shows the molecular weight, magnetic moment coefficient, oxidation state and the geometry of the complex.

Table 2. Magnetic Susceptibility of PTUCo complex

Complex	Mwt	μeef	Shape	Oxidation state
PTUCo	273.623	3.9	tetrahedral	+2

3.5. Mass spectra:

The complex (PTUCo) characterization by mass spectrum technique. Figure 3 Show the molecular ion peak at $[CoC_{10}H_{12}O_4S_2N_4]^+$ which makes the structural formula and molecular weight of the complex and another important peak at 338 m/z can be assigned to the molecular ion $[CoC_{10}H_5O_4S_2N_2]^+$ for the loss of two NH_3 and hydrogen atoms H. and a peak at 324 m/z for the molecular ion $[CoC_{10}H_5O_4S_2N]^+$ is attributed to the loss of the N nitrogen atom from the benzene ring and the beam bundle for the molecular ion $[H_4CoC_2O_4]^+$ at 149 m/z due to the loss of the SCN thiocyanate root. The remainder of the benzene ring, as well as a peak at 104 m/z of the molecular ion $[HCoCO_2]^+$ due to the loss of the CO_2 molecule and two hydrogen atoms, in addition to the emergence of a peak at 57 m/z due to the Co^{2+} cobalt ion. [38].

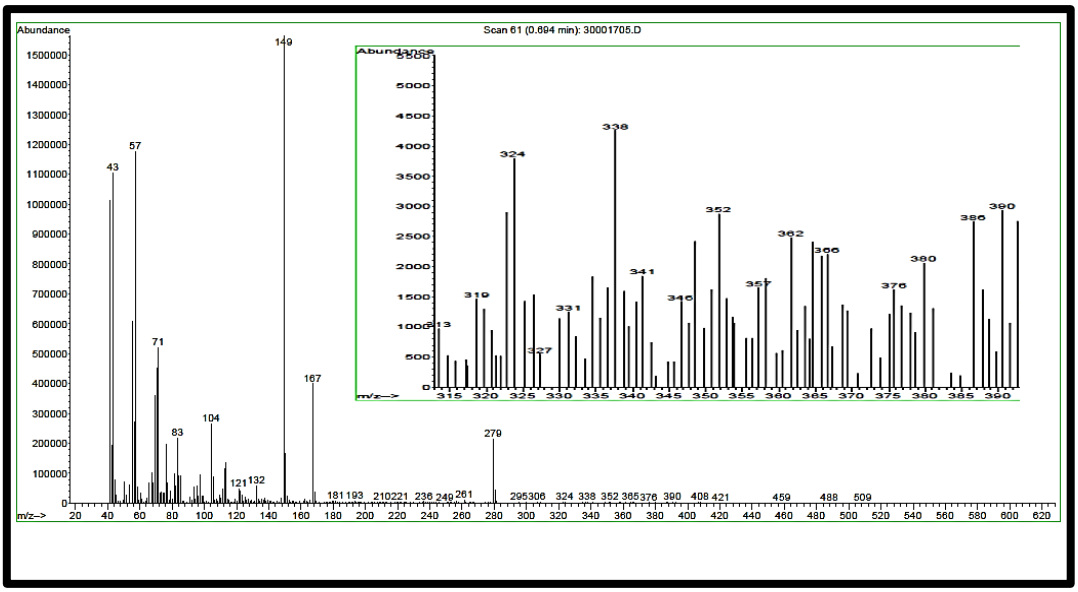

Figure 3: Mass spectrum for PTUCo complex.

3 .6. X-ray Diffraction (XRD):

The complex PTUCo characterized by XRD diffraction as in Figure 4 below where, it was used in the diagnosis of a complex (PTUCo) and the crystal size of the crystallization of the complex was calculated using the (Debye-Scherer) equation[33, 38, 42].

$$D = \frac{K\lambda}{\beta \cos\theta} \dots\dots\dots\dots\dots\dots\dots\dots\dots\dots\dots\dots\dots\dots\dots\dots\dots\dots\dots\dots\dots\dots\dots\dots\dots\dots\dots 1$$

where D is the crystallite size (nm), λ is the x-ray wavelength (0.15406 nm for Cu $K\alpha$), K is the Scherer constant (0.9) that depends on the shape of a crystal, β is the full width at half maximum of intensity, and θ is the Bragg angle, Figure 4 show XRD spectrum for PTUCo with a sharp peak at (2θ=11.8144º),

β =0.00314 radian, D = 44.2374nm. It was observed from the crystal size calculation; the complex has a nano structure.

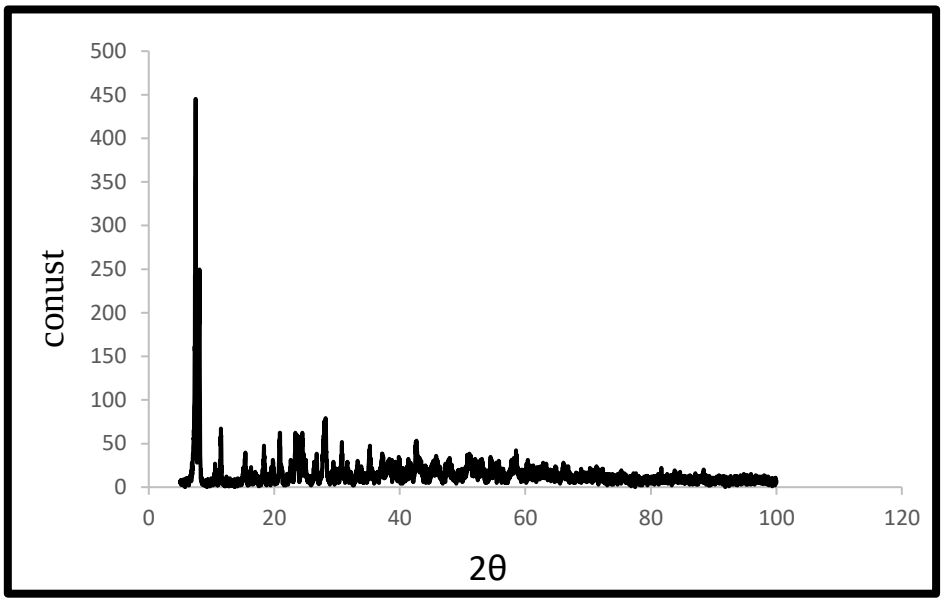

Figure 4: Shows XRD spectrum for PTUCo complex.

3. 7. Thermogravimetric Analysis:

In this study, Thermogravimetric analysis (TGA-DTG) technique was used to study the stability for the complex PTUCo at range of temperatures (25-700 ℃) with a heating rate of 50 ºC/min and the presence of an inert atmosphere of N_2 gas and a flow rate of 30 mL/min. Figure 5 showed TGA-DTG thermogram for PTUCo complex. Through this technique, some thermal functions were calculated, such as the stages of dissociation of the material, the temperature at which the material disintegrates, the rate of dissociation rate, in addition to the remainder after the dissolution process, In Figure (5) the TGA and DTG pyrolysis curve shows the PTUCo complex, it has five phases of dissociation at a temperature of 234.69 ºC, the second at 403.81 ºC and the third at a temperature of 455.70 ℃, while the fourth at a temperature of 553.71 ºC .

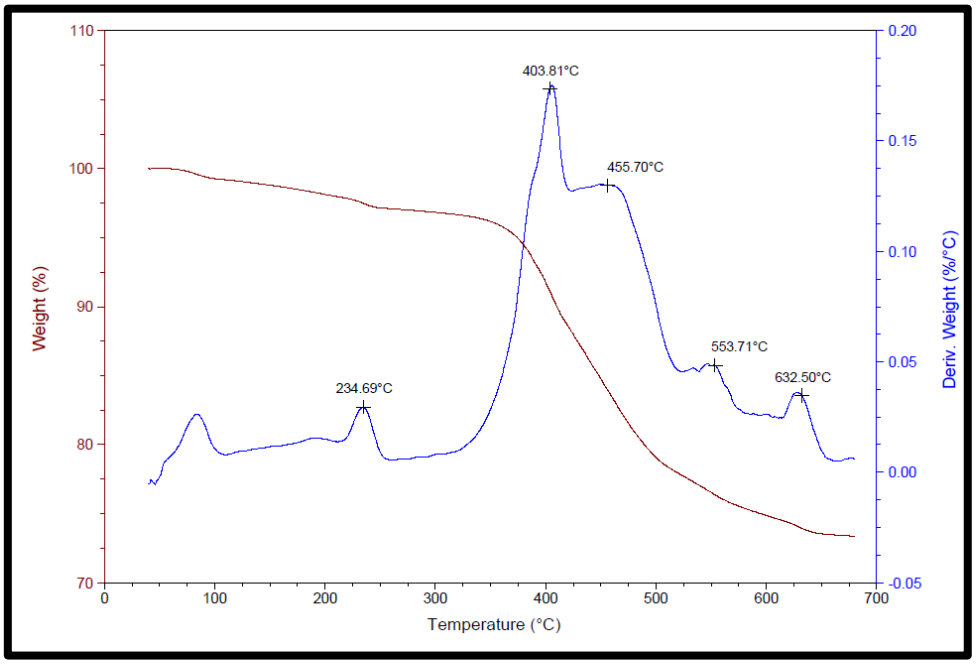

Figure 5: TGA-DTG thermogram for PTUCo complex.

The last one was at a temperature of 632.50 ºC and found that the value of Ts * is at a temperature of 440 ºC and has a char content through the TGA curve or the residue at a temperature of 600 ºC estimated at 75% and the rate of dissociation rate of 1.961%/min, as it is through a curve follow-up TGA at a dissociation rate of approximately 11.78%. The loss of N_2 and H_2 gases from the two ligand thiourea , and at approximately 25% of the loss, there is a loss of carbon monoxide, hydrogen gas and carbon sulfide CS [43, 44].

4. Corrosion study:

The carbon steel alloy employed in this study was C1010 type. The alloy composition is shown in Table 3 below. The composition is obtained by analysis of alloy from university of Basrah, college of engineering.

Table 3. Carbon steel composition (C1010).

Element	C	Mn	Cr	P	S	Cu	Si	As	Ni	Fe
w/w%	0.13	0.30	0.10	0.05	0.04	0.30	0.37	0.08	0.30	Balance

4.1. Preparation of working electrode

Table3 represent the composition of the specimens that used to evaluate (PTUCo) as corrosion inhibitor for carbon steel C1010. the specimens of carbon steel (C1010) was studied as strips with dimensions of (3.1) Cm× (1.15) Cm× (0.15) Cm as length, width and thickness respectively. The dimensions are measured by Vernier with sensitivity of (1) mm. the strips were grinded by silicon carbide with grades 120, 180, 320, 400 and 600 respectively. At each step of grinding the specimen washed by cooling water to reduce the raising in temperature and to prevent the adhesion of the particles of grinding papers taking into account each grinding process is perpendicular on the other to remove any impurities on the alloy surface. Then specimens were washed by water and soap to remove the impurities, and after that the residue of soap was removed by washing with distilled water and ethanol, finally washed by acetone and dried by air to polish by polishing device. The specimen was polished through disc rotator covered by shamwa, alumina Al_2O_3 was added on the polishing disc to polish the sample very well to be smooth as mirror. Then the samples were washed again by distilled water, ethanol and acetone then dried by air. finally, the strips kept in desiccator to prevent them against the moisture.

4.2. Electrochemical cells, potentiodynamic method (Tafel plot), and solution preparation.

In this study, the electrochemical cell in the corrosion test consisted of a 75 mL vessel connected to three electrodes: platinum electrode, carbon steel specimen, and saturated calomel electrode as counter, working, and reference electrodes, respectively. used Five concentrations for PTUCo complex were prepared include (1,2,3,4 and 5) ppm to study the effect of concentration of the complex on the corrosion of surface of C1010 alloy at 25 ºC by using the electrochemical method (Tafel plot method) separately to prepare. The effect of temperature on the corrosion reaction in the presence and absence of optimal and minimal PTUCo concentrations was studied at 25, 35, 45, and 55℃ in 0.1 M HCl as a corrosive agent. Potentiodynamic and polarization measurement is a commonly used technique to measure corrosion resistance and various functions and determine the current density versus the electric potential through a setup of open circuit potential (OCP) for 25 min . The polarization curve can then be acquired by scanning the potential range between −250 mV and +250 mV (vs. OCP) by using a computer for potentiostat/galvanostat at a scanning rate of 10 mV S^{-1}. Various parameters such as corrosion current density (I_{corr}), corrosion potential (E_{corr}), cathodic (β_c) and anodic (β_a). shows a slight drift in the OCP values towards the negative showing the presence of CoPTU inhibitor, this behavior is attributed to adsorption of the inhibitor or/and deposition of the products of the corrosion reaction on the C1010 alloy.

5. Results and discussion

Figure 6 shows Tafel plots for Five concentrations of PTUCo complex relative to blank (corrosive environment of 0.10M of (HCl).

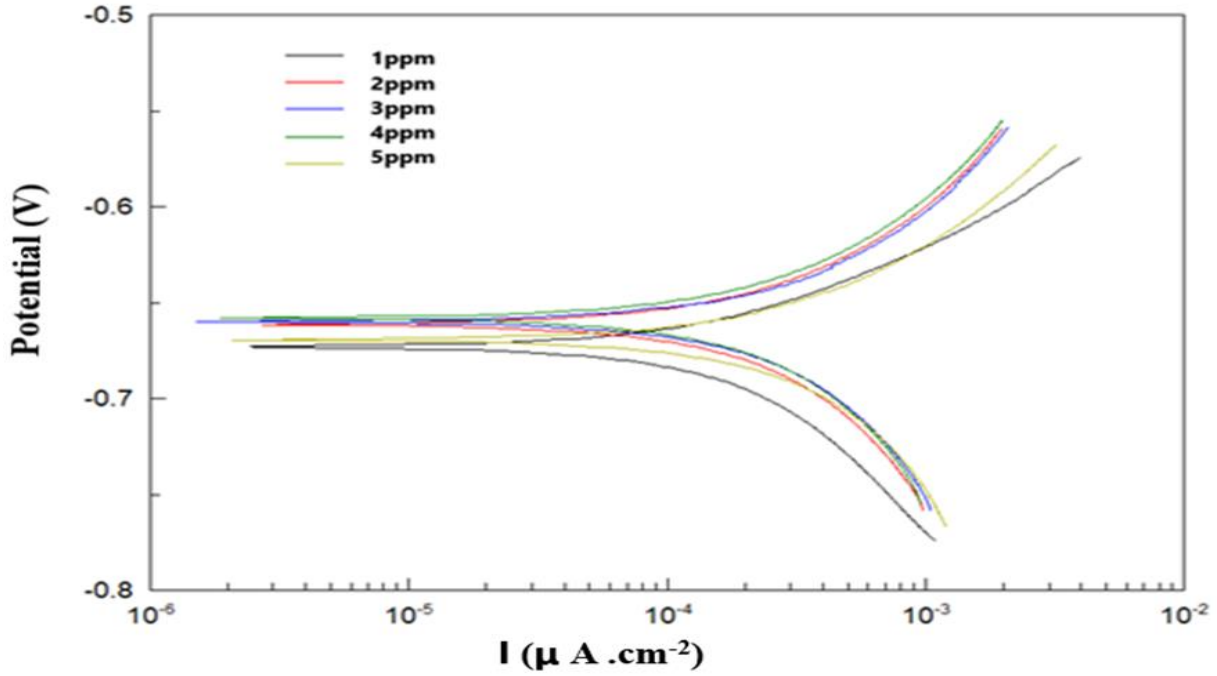

Figure 6: Tafel plots for carbon steel alloy C1010 in presence of different concentration of PTUCo complex at 25 ºC.

The electrochemical data were summarized in Table 4 below.

Table 4: The electrochemical data for the corrosion of C1010 alloy surface in presence of different concentrations of PTUCo relative to blank at 25 ºC.

Comp.	Conc. ppm	E_{corr} mV	β_a mV.decade^{-1}	β_c mV. decade^{-1}	R_{ct} Ω.Cm^2	I_{corr} µA.Cm^{-2}	CR mpy	Effe. %
HCl	3650	- 659	171.27	-333.06	26.28	685.06	317.23	___-
PTUCo	1	- 674	76.61	-147.37	97.37	184.87	85.61	72.96
	2	- 675	474.03	-440.48	357.45	50.36	23.58	92.58
	3	- 677	334.64	-274.71	541.13	33.26	15.40	95.08
	4	- 680	434.49	-366.58	509.66	35.32	16.36	94.77
	5	- 681	424.04	-356.89	610.64	29.48	13.65	95.63

It was depicted from Figure 6 and Table 4, the presence of the complex PTUCo was reduced the corrosion rate for the surface of C1010 alloy at all its concentrations compared with case in presence of blank because the corrosion current density was reduced, the resistance polarization of the alloy was increased as shown in Figure 7, the inhibition efficiency was raised as the concentration of the inhibitor increased to (5) ppm where the damping efficiency is 95.63% [45, 46], the irregular efficiency values between 3ppm to 5ppm concentration can be assigned to is due to the solubility of the inhibitor studied in the acid medium.

Furthermore, the corrosion potential of the alloy in the presence of the corrosive environment E_{corr} is (-659) mV compared with the presence of studied concentrations E_{corr} of the inhibitor values were shifted compared with blank by less than 89mV that indicate the inhibitor behave as mixed inhibitor [47, 48] and both β_a and β_c values were shifted compared with these in blank insisted that the anodic dissolution in anode and hydrogen evolution in cathode were be controlled [49]. It is also possible to suggest that

the high efficiency of inhibition and its convergence within the higher concentrations is due to the complex shape of the complex (PTUCo) which was deduced from magnetic sensitivity calculations as a tetrahedral magnetic bara providing four amine groups (NH_2) and two groups of the thiourea for each complex molecule in addition to the phthalate ion in which Adsorption sites such as benzene ring and the two groups of carbonyl (C = O) as shown in Figure 8 below.

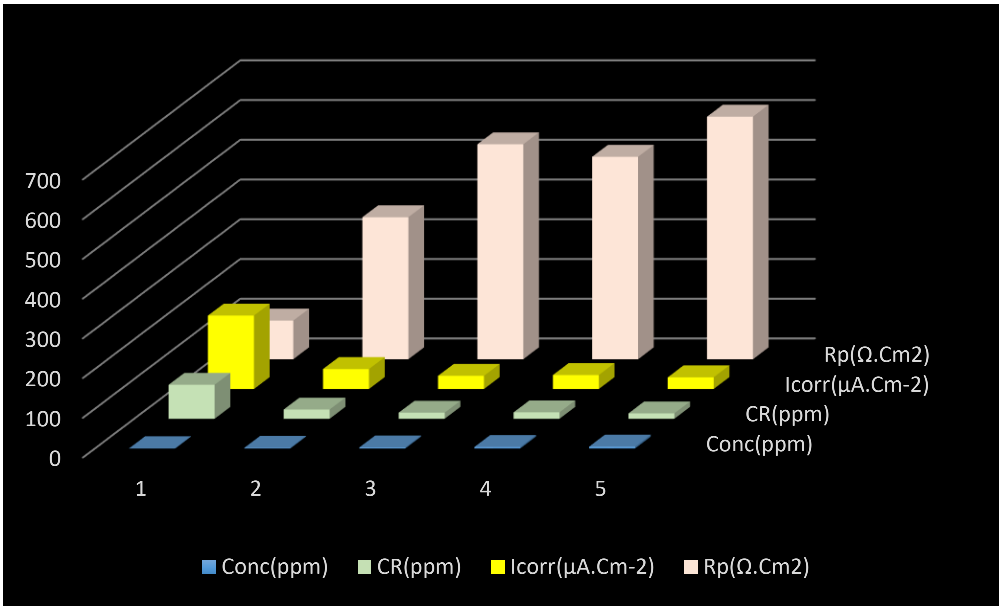

Figure 7: The relation between the concentration of the inhibitors and the electrochemical data for the alloy's surface (C1010).

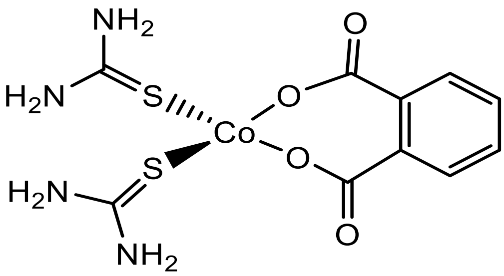

Figure 8: explained the relation between these data and the concentration of the inhibitor.

The efficiency is calculated as in the following equation [50]:

$$effeciency\% = \frac{CR_{uninhib} - CR_{inhib}}{CR_{uninhib}} \times 100 \ldots\ldots\ldots\ldots\ldots\ldots\ldots\ldots\ldots\ldots\ldots\ldots 2$$

Where, $CR_{uninhib}$ and CR_{inhib} are the corrosion rate of the C1010 alloy in the absence and presence of the inhibitors respectively.

5.2. Study the effect of temperature on the corrosion rate of the C1010 alloy:

The effect of temperature on the corrosion reaction on the surface of the mentioned alloy was studied at 298, 308, 318 and 328 K by using Tafel plot methodes at an minimal concentration (1ppm) and at optimal concentration (5ppm). Figures 9, 10 and 11 below depicted Tafel plots for C1010 in absence and presence of a minimal and an optimal concentration of PTUCo as inhibitor. The electrochemical data for these cases were obtained and summerized in Tabel 5 as shown below.

Where, Blank is corrosive environment (0.1M HCl), its concentration in ppm is equal to 3650 ppm. As shown from Table 6, the raising of temperature from 298K (25 ºC) to 328K(55 ºC) the corrosion rate is increased, because the corrosion current increased then, the resistance polarization and inhibition

efficiency of the inhibitor were reduced in both cases (minimal and optimal concentrations) because the protective film of the inhibitor began to dissolved on surface of the alloy where, the corrosive species were attack the surface of. The disparity in efficiencies' values due to the variation of desorption phase relative to the temperature ; a decrease in inhibition efficiencies with the increase in temperature might be due to weakening of physical adsorption sites while retarding the chemisorption sites [51] and a significant decrease is also observed compared to the decrease in efficiency of inhibition using the optimum concentration with increasing temperature within the aforementioned thermal range.

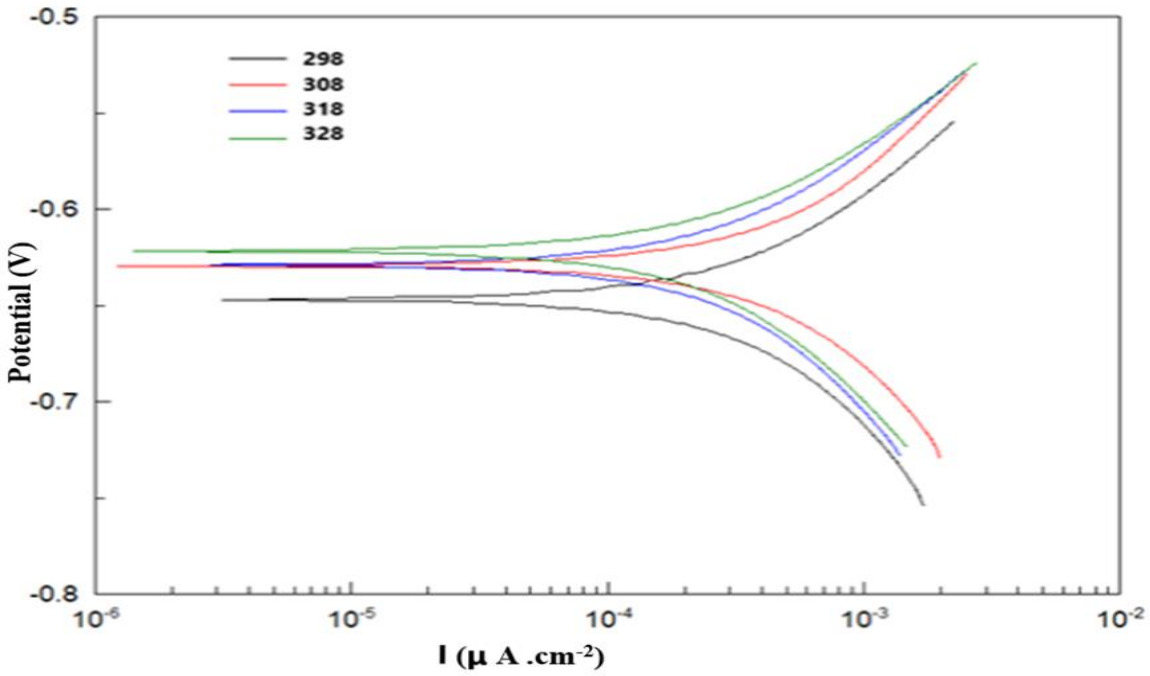

Figure 9: Tafel plots for carbon steel alloy C1010 in presence of corrosive environment of 0.10M HCl at different temperature.

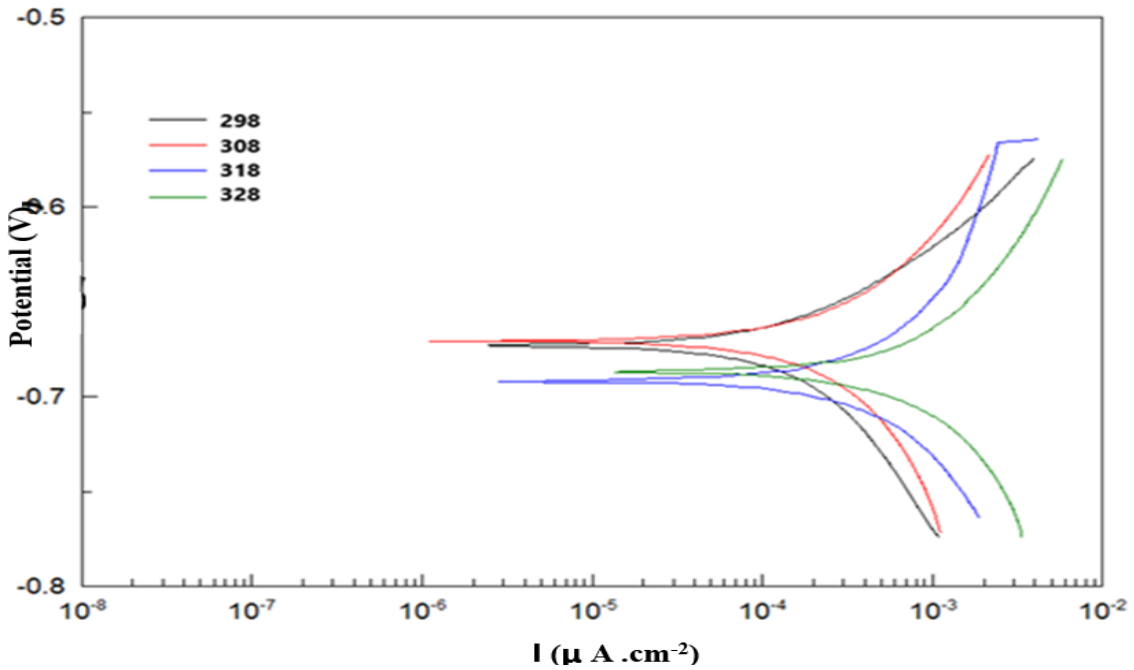

Figure 10: Tafel plots for carbon steel alloy C1010 in presence of the minimal concentration (1ppm) of PTUCo complex at different temperature.

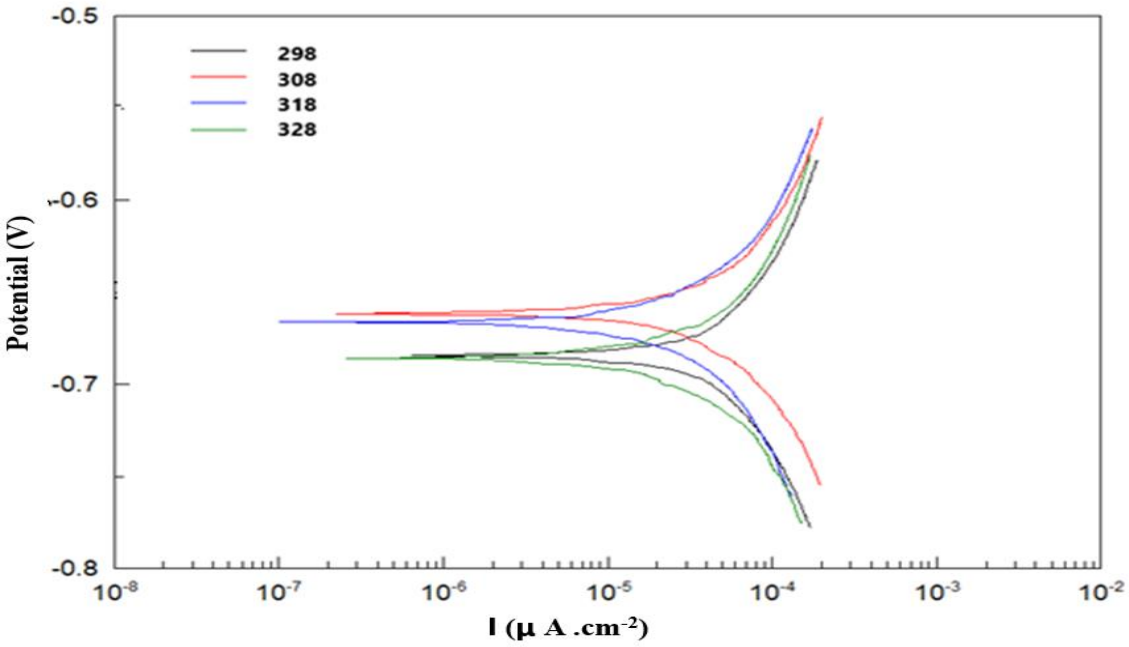

Figure 11: Tafel plots for carbon steel alloy C1010 in presence of the optimal minimal concentration (5ppm) of PTUCo complex at different temperature.

Table 5: The electrochemical data for the corrosion of C1010 alloy surface in presence of minimal concentration (1ppm) and optimal concentration (5ppm) for PTUCo at different temperatures relative to blank.

Comp.	Conc. ppm	Temp. K	E_{corr} mV	β_a mV.decade	β_c mV.decade	R_{ct} Ω.Cm^2	I_{corr} µA.Cm^{-2}	CR mpy	Effe.%	θ
HCl	3650	298	- 659	171.27	-333.06	26.28	685.06	317.23	-	
HCl		308	- 670	370.54	-825.15	21.86	823.32	381.26	-	
HCl		318	- 674	56.45	-186.37	15.87	1132.1	525.16	-	
HCl		328	- 678	193.53	-1165.40	9.41	1912.3	885.45	-	
PTUCo	1	298	- 674	76.61	-147.37	97.37	184.87	85.61	72.96	0.7296
PTUCo	1	308	- 671	161.31	-329.92	73.371	245.33	113.61	70.12	0.7012
PTUCo	1	318	- 691	473.69	-271.22	40.978	439.26	203.41	61.13	0.6113
PTUCo	1	328	- 687	130.81	-133.44	22.49	800.34	370.62	58.18	0.5818
PTUCo	5	298	- 681	424.04	-356.89	610.64	29.48	13.65	95.63	0.9563
PTUCo	5	308	- 676	187.35	-217.51	86.17	208.88	96.79	74.53	0.7453
PTUCo	5	318	- 681	409.59	-430.11	51.89	346.88	160.63	69.26	0.6926
PTUCo	5	328	- 691	156.92	-785.45	22.04	816.82	378.29	57.31	0.5731

Therefore, it is preferable to use the optimal concentration of inhibitor (PTUCo) with an optimal concentration of (5) ppm and is observed in both the two cases of the values of the Tafel anode and cathode constants are that they are in a change and fall indication of a decrease in the control mechanisms of the anode and cathode reactions [45, 52]. One of the values of corrosion efforts is that the inhibitor is still conducting a double inhibitor even with a high temperature. in Figure 12 the effect of temperature on corrosion rate and other electrochemical parameters can be shown.

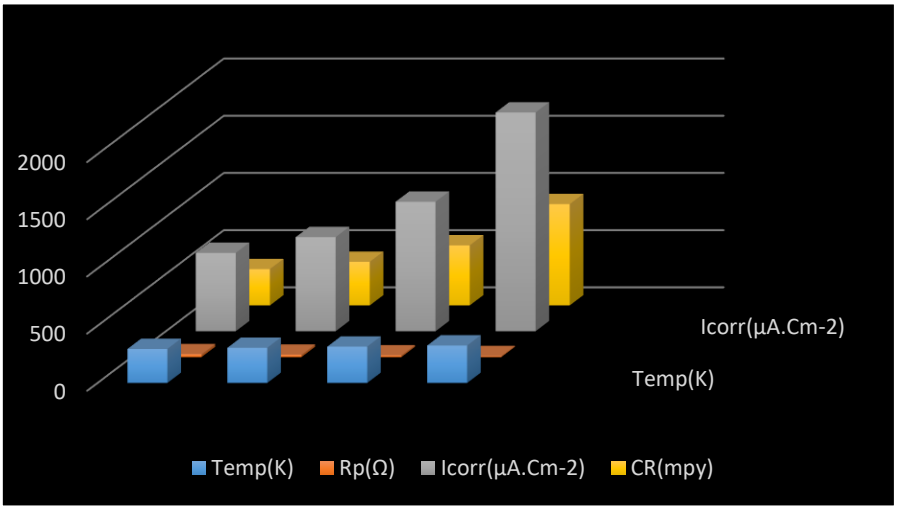

Figure 12: The effect of temperature on the electrochemical parameters on the 1010 alloy in absence of the inhibitor.

5.6. Calculation of kinetic parameters for corrosion reaction of alloy:

In this study, kinetic parameters like activation of energy E_a^* in kJ.mol^{-1} , enthalpy of activation ΔH^* in kJ.mol^{-1} and entropy of activation ΔS^* in J.K^{-1}.mol^{-1} were calculated for the optimal and minimal concentrations to explain the behavior of corrosion reaction on the alloy in presence and absence of the inhibitor. Firstly, activation energy was calculated according to Arrhenius equation as in equation 8 below [9, 53, 54]:

$$\ln CR = \ln A - \frac{E_a^*}{RT} \quad \text{.....3}$$

Where, A is Arrhenius Pre-exponential and CR is corrosion rate in pmy. Thus, plotting the relationship between $\ln CR$ against $\frac{1}{T}$ to give a straight line with slope equal to $(-\frac{E_a^*}{R})$ as in Figure 13 below:

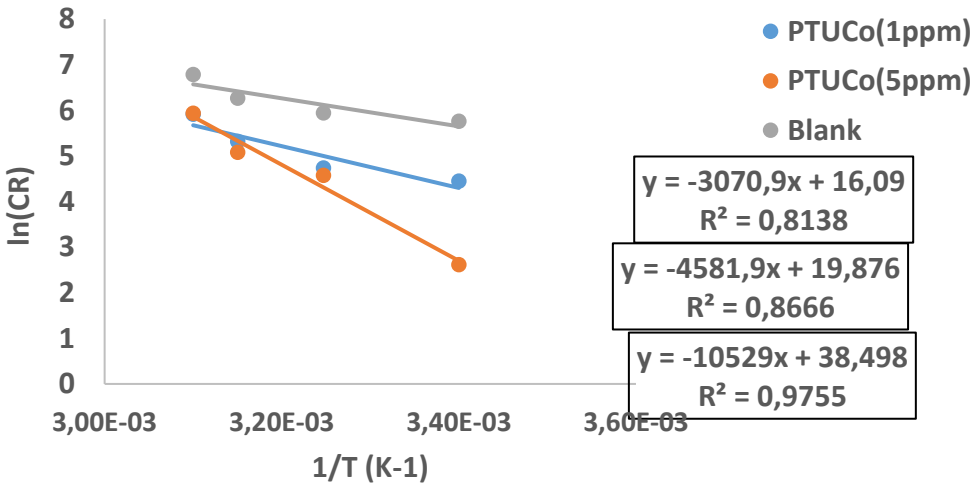

Figure 13: Arrhenius relationship for the corrosion reaction on the surface of C1010 alloy in absence and presence of 1 and 5 ppm of PTUCo.

The enthalpy and entropy of activation were calculated as in equation 9 below [52, 54, 55]:

$$\ln(\frac{CR}{T}) = \ln\frac{R}{Nh} + \frac{\Delta S^*}{R} - \frac{\Delta H^*}{RT} \quad \text{.....4}$$

Where, N is Avogadro's number is equal to n$6.023 \times 10^{23} mol^{-1}$ and h is Plank's constant is equal to $6.625 \times 10^{-34} J.s$. thus, plotting of $\ln(\frac{CR}{T})$ against $\frac{1}{T}$ give a straight line, its slope equal to $\frac{-\Delta H^*}{R}$ and the intercept equal to $(\ln\frac{R}{Nh} + \frac{\Delta S^*}{R})$ as in Figures 14 and 15 below :

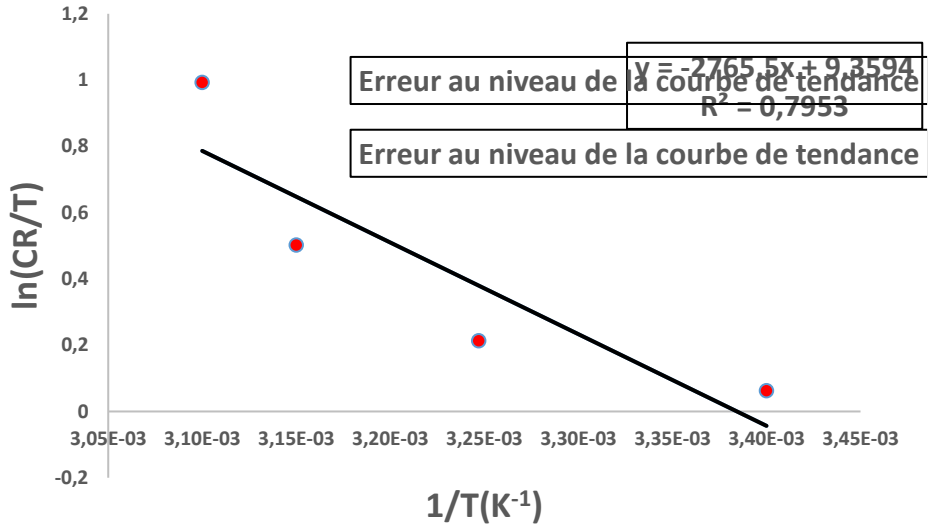

Figure 14: calculation of enthalpy and entropy of activation for the corrosion reaction on the surface of C1010 alloy in presence of corrosive environment only.

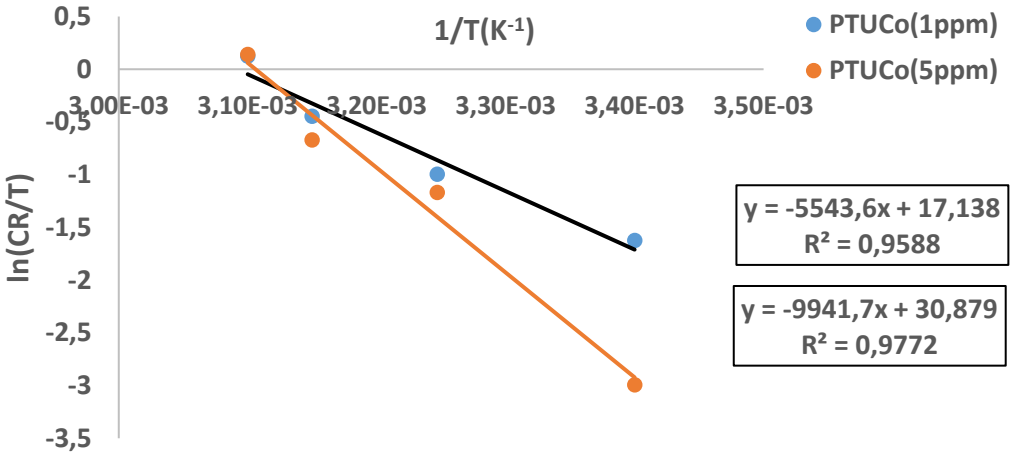

Figure 15: calculation of enthalpy and entropy of activation for the corrosion reaction on the surface of C1010 alloy in absence and presence of 1 and 5 ppm of PTUCo.

The kinetic parameters were summarized in Table 7 below:

Table 7: Kinetic parameters for the corrosion reaction on the surface of C1010 alloy in absence and presence of PTUCo inhibitor.

Comp.	Conc. ppm	E_a kJ.mol^{-1}	A s^{-1}	ΔH* kJ.mol^{-1}	ΔS* J.mol^{-1}.K^{-1}	ΔG* kJ.mol^{-1}
HCl	3650	25.53	9.72×10^{6}	22.99	-119.73	58.67
PTUCo	1	38.09	4.29×10^{8}	46.09	-55.06	62.50
	5	87.54	5.24×10^{16}	82.66	59.19	65.02

Table 7 depicted that the energy of activation in presence of PTUCo inhibitor is greater than in absence of inhibitor especially in presence of optimal concentration (5ppm), which means that the corrosion reaction of the carbon steel iron alloy in the absence of the inhibitor is fast compared with the presence of the inhibitor. Furthermore, in case of presence the optimal concentration, the corrosion reaction became very slow that corresponding with the higher damping efficiency than in case of a minimal

concentration i.e., the inhibition of the optimal inhibitor on the alloy surface was forming a higher protective layer on the surface of the alloy [56, 57]. On the other hand, the enthalpy of activation corrosion reaction ΔH* values were positive and increased in presence of the inhibitor especially in case of the optimal concentration that confirm the dropping of the inhibition efficiencies as the temperature was raised. This confirms that the process of adsorption of inhibitor is more chemical than physical, in other words that the chemical desorption separation needs to heat to get faster [50, 58]. It is also noticed through Table 7 that the values of the Arrhenius coefficient (A) increase with the presence of the inhibitor, especially at the optimal concentration, it is worth noting that the Arrhenius coefficient indicates the coefficient of vibration of the interacting particles i.e., the corrosive species and the surface of alloy in absence of the inhibitor, this coefficient was raised in the presence of the inhibitor that can be attributed to the increasing the vibration of the reaction system i.e., (corrosion product (none porous hydrated iron oxide), inhibitor molecules and the surface of alloy) to form the activated complex which tends to form a protective layer [53,54]. On the other hand, the values of the activation entropy is negative in case of absence the inhibitor (-119.73) $J.mol^{-1}.K^{-1}$ means that the corrosion products tends to be stable and regular on the surface of alloy. The negative value then tends to be reduced in case of the presence of a minimal concentration (-55.06) $J.mol^{-1}.K^{-1}$ reached to be positive value (59.19) $J.mol^{-1}.K^{-1}$ when the optimal concentration of the inhibitor is present on the surface of alloy, this can be attributed to increase the instability of corrosion products when the certain inhibitor was adsorbed on the surface of alloy causing the increasing the entropy to combine between each other i.e., the process of adsorption of the inhibitor affects the corrosion reaction by expelling the larger number of corrosive molecules with water molecules, which increases the randomness of the reaction, leading to the formation of an adsorbent layer that reduces the corrosion process [58-60].

Conclusions

The cobalt complex (PTUCo) has a tetrahedral geometrical shape paramagnetic, which confirms the replacement of two ligands from thiourea versus the one ligand of the phthalate ion. The synthesized complex PTUCo can be used as corrosion inhibitor for corrosive environment of 0.10M of HCl at very little concentration i.e., 5 ppm with efficiency 95.63%. Its behavior is mixed inhibitor. Where, the inhibitor PTUCo raised the activation energy for the corrosion reaction on the surface of C1010 alloy. The mechanism of hydrogen evolution in the cathode and anodic dissolution in the anode were controlled in presence of this inhibitor.

References

1. I. Benmahammed, T. Douadi , S. Issaadi, N. AL-Noaimi, S. chafaa, Heterocyclic Schiff bases as corrosion inhibitors for carbon steel in 1 M HCl solution: hydrodynamic and synergetic effect. *Journal of Dispersion Science and Technology*, 41 (2019) 1-20.
2. L.O.O. Lasunkanmi, M.M. Kabanda, E.E. Ebenso, Quinoxaline derivatives as corrosion inhibitors for mild steel in hydrochloric acid medium: Electrochemical and quantum chemical studies. *Physica E: Low-dimensional Systems and Nanostructures*, 76 (2016) 109-126.
3. H.M.A. AL-Lateff, A.M. Abu-Dief, M.A. Mohamed, Corrosion inhibition of carbon steel pipelines by some novel Schiff base compounds during acidizing treatment of oil wells studied by electrochemical and quantum chemical methods. *J. Molecular Structure*, 1130 (2017) 522-42
4. M. Jeeva, G. V. Prabhu , M.S. Boobalan, C.M. Rajesh, Interactions and inhibition effect of urea-derived Mannich bases on a mild steel surface in HCl. *The Journal of Physical Chemistry C*, 119(38) (2015) 22025-22043.

5. A. Döner, R. Solmaz, M. Özcan, G. Kardaş, Experimental and theoretical studies of thiazoles as corrosion inhibitors for mild steel in sulphuric acid solution. *Corrosion Science*, 53 (2011) 2902-2913
6. H.M.A. El-Lateef, M.S.S. Adam, M.M. Khalaf, Synthesis of polar unique 3d metal-imine complexes of salicylidene anthranilate sodium salt. Homogeneous catalytic and corrosion inhibition performance. *Journal of the Taiwan Institute of Chemical Engineers*, 88 (2018) 286-304
7. Z.N. Kadhima, M.A. Mahadia, H.Z. Al-Sawaada, Synthesis, characterization and corrosion inhibitors Evaluation of some Schiff base complexes of Copper (II), and Molybdenum (VI) *International Journal of Academic Studies* , 2(11) (2016) 446-463.
8. A. Biswas, D. Das, H. Lgaz, S. Pal, U.G. Nair, Biopolymer dextrin and poly (vinyl acetate) based graft copolymer as an efficient corrosion inhibitor for mild steel in hydrochloric acid: electrochemical, surface morphological and theoretical studies. *Journal of Molecular Liquids*, 275 (2019) 867-878.
9. A.A. Khadom, Effect of temperature on corrosion inhibition of copper-nickel alloy by tetraethylene pentamine under flow conditions. *Journal of the Chilean Chemical Society*, 59(3) (2014) 2545-2549
10. Yadav, M., et al., Corrosion inhibitive effect of synthesized thiourea derivatives on mild steel in a 15% HCl solution. *International Journal of Electrochemical Science*, 9(11) (2014) 6529-6550.
11. Y. ELouadi, F. Abrigach, A. Bouyanzer, R. Touzani, O. Riant, B. ElMahi, A. El Assyry, S. Radi, A. Zarrouk and B. Hammouti. Corrosion inhibition of mild steel by new N-heterocyclic compound in 1 M HCl: Experimental and computational study. *Der Pharma Chemica*, 7 (8) (2015) 265-275.
12. Y. El Ouadi, M. Elfal, A. Bouyanzer, H. Elmsellem, Y. Ramli, E.M. Essassi, N. Lahhit, A. Aouniti, A. Chetouani and B. Hammouti. Effect of 1,5-dibenzyl-1H-pyrazolo [3,4-d] pyrimidine-4 (5H) - thione on inhibition of mild steel corrosion in 1M HCl. *Der Pharma Chemica*, 7(9) (2015) 354-367.
13. K. Cherrak, A. Dafali, A. Elyoussfi, Y. El Ouadi, N. K. Sebbar, M. El Azzouzi, H. Elmsellem, E. M. Essassi, A. Zarrouk. Two new benzothiazine derivatives as corrosion inhibitors for mild steel in hydrochloric acid medium. *J. Mater. Environ. Sci.*, 8, Issue 2 (2017) 636-647.
14. Y. El Ouadi, H. Elmsellem, M. El fal, N.K. Sebbar, A. Bouyanzer, R. Rmili, E.M. Essassi, B. El Mahi, L. Majidi, B. Hammouti. Effect of 1,5-di (prop-2-ynyl)-1H-pyrazolo[3,4-d]pyrimidine-4 (5H) - thione on inhibition of mild steel corrosion in 1M HCl. *Der Pharma Chemica*, 8(1) (2016) 365-373.
15. Y. El Ouadi, F. Abrigach, A. Bouyanzer, R. Touzani, A. El Assyry, A. Zarrouk, B. Hammouti. Theoretical and Experimental Studies on the Corrosion Inhibition Potentials of Two Tetrakis Pyrazole Derivatives for Mild Steel in 1.0 M HCl. *Portugaliae Electrochimica Acta*, 35 (3) (2017) 159-178.
16. I. Merimi, Y. El Ouadi, K. Rahmani Ansari, H. Oudda, B. Hammouti, M. A. Quraishi, F. F. Al-blewi, N. Rezki, M. R. Aouad and M. Messali. Adsorption and Corrosion Inhibition of Mild Steel by ((Z)-4-((2,4-dihydroxybenzylidene) amino)-5-methy-2,4 dihydro-3H-1,2,4-triazole-3-thione) in 1M HCl: Experimental and Computational Study. *Anal. Bioanal. Electrochem.*, 9 (2017) 640-659.
17. M. El Azzouzi, A. Aouniti, M. El-massaoudi, S. Radi, B. Hammouti, A. Quraishi, H. Bendaif, Y. El Ouadi. Inhibition effect of 1,1´-(pyridine-2,6-dihylbis(methylene))bis(5-methyl-1-H-pyrazole-3-carboxylic acid) on the corrosion of mild steel in 1 M HCl. Part A: Experimental study. *Int. J. Corros. Scale Inhib.*, 6, no. 4 (2017) 463-475.
18 I. Merimi, Y. EL Ouadi, R. Benkaddour, H. Lgaz, M. Messali, F. Jeffali and B. Hammouti. Improving corrosion inhibition potentials using two triazole derivatives for mild steel in acidic medium: Experimental and theoretical studies. *Materials Today: Proceedings* 13 (2019) 920–930.

19. Y. El Ouadi, M. El Fal, B. Hafez, M. Manssouri, A. Ansari, H. Elmsellem, Y. Ramli, H. Bendaif, Physisorption and corrosion inhibition of mild steel in 1 M HCl using a new pyrazolic compound : Experimental data & quantum chemical calculations, *Materials Today: Proceedings* 27 (2020) 3010-3016. https: //doi.org/10.1016/j.matpr.2020.03.340.
20. H.Z. Al-Sawaad, Z.N. Kadhim, M.A. Mahadi, Evaluation of Schiff Base Complex of Copper (II) as Corrosion Inhibitor against 0.1 M of Hydrochloric Acid. *Journal of Chemical and Pharmaceutical Research*, 8(9) (2016) 150-163.
21. P. Singh, A.K. Singh, V.P. Singh, Synthesis, structural and corrosion inhibition properties of some transition metal (II) complexes with o-hydroxyacetophenone-2-thiophenoylhydrazone. *Polyhedron*, 65 (2013) 73-81.
22. K.M. Takroni, H.A. El-Ghamry, A. Fawzy, Evaluation of the Catalytic Activities of Some Synthesized Divalent and Trivalent Metal Complexes and Their Inhibition Efficiencies for the Corrosion of Mild Steel in Sulfuric Acid Medium. *Journal of Inorganic and Organometallic Polymers and Materials*, (2019) 1-14.
23. M. Rbaa, A.S. Abousalem, M. Ebn Touhami, Novel Cu(II) and Zn(II) complexes of 8-hydroxy-quinoline derivatives as effective corrosion inhibitors for mild steel in 1.0 M HCl solution: Computer modeling supported experimental studies. *Journal of Molecular Liquids*, (2019) 111243.
24. W. Gou, W. Wang, X. Weenrong,P. Zhang, L. Wang, J. Zhang, Y. Shi, B. Xie, Study on Thermal Stability and Corrosion Inhibition Effect of [Ni (s-htde)](ClO4) 2 for Q235 Steel in 1.0 M HCl. *Int. J. Electrochem. Sci*, 14 (2019) 7947-7960.
25. M. Mishra, T. Karishma, M. Punita, S.MM, S. Punita, Synthesis characterization and corrosion inhibition property of nickel (II) and copper (II) complexes with some acylhydrazine Schiff bases. *Polyhedron*, 89 (2015) 29-38.
26. K.S. Lokesh , M.D. Keersmaecker, A. Elia, D. Depla, P. Dubruel, P. Vandenabeele, S.V. Vlierberghe, A. Adriaens, Adsorption of cobalt (II) 5, 10, 15, 20-tetrakis (2-aminophenyl)-porphyrin onto copper substrates: Characterization and impedance studies for corrosion inhibition. *Corrosion science*, 62 (2012) 73-82.
27. X. Liu,Y. Lu, Y. Yang, H.X. Hu, Y.G. Zheng, Electrochemical behavior of phenylalanine and its cobalt complex as corrosion inhibitors for mild steel in H_2SO_4. *Russian Journal of Applied Chemistry*, 88(2) (2015) 350-355.
28. C.B. Shen, S.G. Wang, H.Y. Yng, K.Long, F.H. Wang, Corrosion and corrosion inhibition by thiourea of bulk nanocrystallized industrial pure iron in dilute HCl solution. *Corrosion science*, 48(7) (2006) 1655-1665.
29. D. Q. Huong, T. Duong, P.C. Nam, Effect of the Structure and Temperature on Corrosion Inhibition of Thiourea Derivatives in 1.0 M HCl Solution. *ACS omega*, 4(11) (2019) 14478-14489.
30. P.A. Ajibade, N.H. Zulu, *Metal complexes of diisopropylthiourea: Synthesis, characterization and antibacterial studies.* International journal of molecular sciences, 12(10) (2011) 7186-7198.
31. G. Binzet, G. Kavak, N. Külcü, S. Özbey, U. Flörke, H. Arslan, Synthesis and characterization of novel thiourea derivatives and their nickel and copper complexes. *Journal of Chemistry*, 2013. 2013
32. N.I.M. Halim, K. Kaasim, A.H. Fadzil, B.M. Yamin, Sintesis, pencirian dan kajian aktiviti antibakteria kompleks Cu (II) tiourea. *Malaysian Journal of Analytical Sciences*, 16(1) (2012) 56-61
33. O.A. El-Gammal, A.E.-A.S. Fouda, D.M. Nabih, Novel Mn^{2+}, Fe^{3+}, Co^{2+}, Ni^{2+} and Cu^{2+} complexes of potential OS donor thiosemicarbazide: Design, structural elucidation, anticorrosion potential study and antibacterial activity. *Journal of Molecular Structure*, 1204 (2020)127495.

34. C. Rao, R. Venkataraghavan, T. Kasturi, Contribution to the infrared spectra of organosulphur compounds. *Canadian journal of chemistry*, 42(1) (1964) 36-42.
35. S.A. Zakaria, S.H. Muharam, M.S.M. Yusof, W.M. Khairul, M.A. kadir, B.M. Yamin, Spectroscopic and structural study of a series of pivaloylthiourea derivatives. *Malaysian Journal of Analytical Sciences*, 15(1) (2011) p. 37-45.
36. K.G. Akpomie, O.M. Famyomi, C.C. Ezeofor, R.S. Ato, W.E.V. Zyl, Insights into the use of metal complexes of thiourea derivatives as highly efficient adsorbents for ciprofloxacin from contaminated water. *Transactions of the Royal Society of South Africa*, 74(2) (2019) 180-188.
37. M. Sonmez, Synthesis and characterization of copper (II), nickel (II), cadmium (II), cobalt (II) and zinc (II) complexes with 2-benzoyl-3-hydroxy-1-naphthylamino-3-phenyl-2-propen-1-on. *Turkish Journal of Chemistry*, 25(2) (2001) 181-186.
38. O.B. Ibrahim, Complexes of urea with Mn (II), Fe (III), Co (II), and Cu (II) metal ions. *Advances in Applied Science Research*, 3(6) (2012) 18.
39. K. Ghazal, S. Shoaib, M. Khan, S. Khan, M.K. Rauf, N. Khan, A. Badshah, M.N. Tahir, I. Ali, A-ur-Rehman, Synthesis, characterization, X-ray diffraction study, in-vitro cytotoxicity, antibacterial and antifungal activities of nickel (II) and copper (II) complexes with acyl thiourea ligand. *Journal of Molecular Structure*, 1177 (2019) 124-130.
40. M.S. Refat, I.M. EL-Deen, M.A. Zein, A.A.Abdel Majid, K.I. Mohamed, Spectroscopic, structural and electrical conductivity studies of Co (II), Ni (II) and Cu (II) complexes derived from 4-acetylpyridine with thiosemicarbazide. *International Journal of Electrochemical Science*, 8(7) (2013) 9894-9917.
41. S. San Tan, A.A. AL-abbasi, M.I.M. Tahir, M.B. Kassim, Synthesis, structure and spectroscopic properties of cobalt (III) complexes with 1-benzoyl-(3, 3-disubstituted) thiourea. *Polyhedron*, 68 (2014) 287-294.
42. A. Monshi, M.R. Foroughi, M.R. Monshi, Modified Scherrer equation to estimate more accurately nano-crystallite size using XRD. *World journal of Nano Science and Engineering*, 2(3) (2012) 154-160.
43. S.T. Breviglieri, É.T.G. Cavalheiro, G.O. Chierice, Correlation between ionic radius and thermal decomposition of Fe (II), Co (II), Ni (II), Cu (II) and Zn (II) diethanoldithiocarbamates. *Thermochimica acta*, 356(1-2) (2000) 79-84.
44. A.K. El-Sawaf, F. El-Essawy, A.A. Nassar, Elsayed A. El-samanody, Synthesis, spectral, thermal and antimicrobial studies on cobalt (II), nickel (II), copper (II), zinc (II) and palladium (II) complexes containing thiosemicarbazone ligand. *Journal of Molecular Structure*, 1157 (2018) 381-394
45. B. Devika, B. Doreswamy, H. Tandon, Corrosion behaviour of metal complexes of antipyrine based azo dye ligand for soft-cast steel in 1 M hydrochloric acid. *Journal of King Saud University-Science*, 32(1) (2020) 881-890.
46. C.M. Fernandes, L.X. Alvarez, N.E. Santos, A.C.M. Barrios, E.A. Ponzio, Green synthesis of 1-benzyl-4-phenyl-1H-1,2,3-triazole, its application as corrosion inhibitor for mild steel in acidic medium and new approach of classical electrochemical analyses. *Corrosion Science*, 149 (2019) 185-194.
47. M. Manssouri, Y. El Ouadi, M. Znini, J. Costa, A. Bouyanzer, J-M. Desjobert, L. Majidi, Adsorption proprieties and inhibition of mild steel corrosion in HCl solution by the essential oil from fruit of Moroccan Ammodaucus leucotrichus. *J. Mater. Environ. Sci.*, 6(3) (2015) 631-646.

48. H.H. Radey, M.N. Khalaf, H.Z. Al-Sawaad, Novel Corrosion Inhibitors for Carbon Steel Alloy in Acidic Medium of 1N HCl Synthesized from Graphene Oxide. *Open Journal of Organic Polymer Materials*, 8(04) (2018) 53.
49. H.Z. AL-Sawaad, Evaluation of the ceftriaxone as corrosion inhibitor for carbon steel alloy in 0.5 M of hydrochloric acid. *Int. J. Electrochem. Sci*, 8 (2018) 3105-3120.
50. M. Larouj, K. Ourrak, M. El M'Rabet, H. Zarrok, H. Serrar, M. Boudalia, S. Boukhriss, I. Warad, H. Oudda, R. Touir, Thermodynamic study of corrosion inhibition of carbon steel in acidic solution by new pyrimidothiazine derivative. *J. Mater. Environ. Sci.*, 8(11) (2017) 3921-3931.
51. M. Lebrini, F. Robert, C. Roos, Adsorption properties and inhibition of C38 steel corrosion in hydrochloric solution by some indole derivates: temperature effect, activation energies, and thermodynamics of adsorption. *International Journal of Corrosion*, 2013. 2013.
52. H.Z. Al-Sawaad, N.T. Faili, A.H. Essa, Evaluation of Vicine as a Corrosion Inhibitor for Carbon Steel Alloy. *Portugaliae Electrochimica Acta*, 37(4) (2019) 205-216.
53. A.M.A. Al-Sammarraie, M. H. Raheema, Electrodeposited reduced graphene oxide films on stainless steel, copper, and aluminum for corrosion protection enhancement. *International Journal of Corrosion*, 2017. 2017.
54. S.A. Rao, P. Rao, Corrosion inhibition and adsorption behavior of Murraya koenigii extract for corrosion control of aluminum in hydrochloric acid medium. *Surface Engineering and Applied Electrochemistry*, 53(5) (2017) 475-485.
55. A.A. Naser, H.Z. Al-Sawaad, A.S. Al-Mubarak, Novel graphene oxide functionalization by urea and thiourea, and their applications as anticorrosive agents for carbon steel alloy in acidic medium. *J. Mater. Environ. Sci.*, 11(3) (2020) 404-420
56. P. Dave, C. LV, Schiff based corrosion inhibitors for metals in acidic environment: A review. *Material Sci & Eng*, 2(6) (2018) 258-267.
57. R.N. El-Tabesh, A.M. Abdl-Gaber, H.H. Hammud, R. Oweini, Effect of Mixed-Ligands Copper Complex on the Corrosion Inhibition of Carbon Steel in Sulfuric Acid Solution. *Journal of Bio-and Tribo-Corrosion*, 6(2) (2020) 29.
58. N.I. Kairi, J. Kassim, The effect of temperature on the corrosion inhibition of mild steel in 1 M HCl solution by Curcuma longa extract. *International Journal of Electrochemical Science*, 8(5) (2013) 7138-7155.
59. O.A. Akinbulumo, O.J. Odejobi, E.L. Odekanle, Thermodynamics and adsorption study of the corrosion inhibition of mild steel by Euphorbia heterophylla L. extract in 1.5 M HCl. *Results in Materials*, 5 (2020) 100074.
60. B. Prasanna, et al., Electrochemical study on inhibitory effect of Aspirin on mild steel in 1 M hydrochloric acid. *Journal of the Association of Arab Universities for Basic and Applied Sciences*, 22 (2017) 62-69.

(2020) ; http://www.jmaterenvironsci.com